JPET Fast Forward. Published on April 12, 2017 as DOI: 10.1124/jpet.116.238840
This article has not been copyedited and formatted. The final version may differ from this version.

Selective calcium-dependent inhibition of ATP-gated P2X3 receptors by bisphosphonates-induced endogenous ATP analogue ApppI

Yevheniia Ishchenko, Anastasia Shakirzyanova, Raisa Giniatullina, Andrei Skorinkin, Genevieve Bart, Petri Turhanen, Jorma A Määttä, Jukka Mönkkönen and Rashid Giniatullin

Author affiliations:

A. I. Virtanen Institute University of Eastern Finland (Y.I., A.Sh., Rai.G., G.B., R.G.), Kazan Institute of Biochemistry and Biophysics Russia (A.S., A.Sh.), School of Pharmacy University of Eastern Finland (P.T., J.M.), Institute of Biomedicine University of Turku Finland (J.A.M.), Kazan Federal University Russia (A.Sh., A.S., R.G.)

Running tittle: ApppI inhibits P2X3 receptors

Corresponding author: Rashid Giniatullin, A.I. Virtanen Institute, University of Eastern Finland, FI-70211 P.O.Box 1627 (Neulaniementie 2) Kuopio Finland, Tel: +358 40 355 3665; Fax: +358 17 163 030; E-mail: rashid.giniatullin@uef.fi.

Number of text pages: 27

Number of tables: 0

Number of figures: 9

Number of references: 67

Number of words in the abstract: 250

Number of words in the introduction: 730

Number of words in the discussion: 872

List of non-standard abbreviations:

ApppI – 1-adenosin-5'-yl ester 3-(3-methylbut-3-enyl) triphosphoric acid diester;

IPP – isopentenyl pyrophosphate;

NBP – nitrogen-containing bisphosphonates;

non-NBP – nitrogen free bisphosphonates.

rP2X – rat P2X

hP2X – human P2X

Recommended section assignment: Neuropharmacology

Abstract

Pain is the most unbearable symptom accompanying primary bone cancers and bone metastases. Bone resorptive disorders are often associated with hypercalcemia contributing to the pathological process. Nitrogen-containing bisphosphonates (NBP) are efficiently used to treat bone-cancers and metastases. NBP, apart from their toxic effect on cancer cells, also provide analgesia via poorly understood mechanisms. We have previously shown, that NBP, by inhibiting the mevalonate pathway, induced the formation of the novel ATP-analogues such as ApppI which can potentially be involved in NBP analgesia. In this study, we used patch-clamp technique to explore the action of ApppI on native ATP-gated P2X receptors in rat sensory neurons and rat and human P2X3, P2X2 and P2X7 receptors expressed in HEK cells. We found, that while ApppI has weak agonist activity, it is a potent inhibitor of P2X3 receptors operating in the nanomolar range. The inhibitory action of ApppI was completely blocked in hypercalcemia-like conditions and was stronger on human than on rat P2X3 receptors. In contrast, P2X2 and P2X7 receptors were insensitive to ApppI, suggesting a high selectivity of ApppI for the P2X3 receptor subtype. NBP, metabolite IPP and endogenous AMP, did not exert any inhibitory action indicating that only intact ApppI has inhibitory activity. The Ca^{2+}-dependent inhibition was stronger in trigeminal neurons preferentially expressing desensitizing P2X3 subunits than in nodose ganglia neurons, which also express non-desensitizing P2X2 subunits. Altogether, we characterized previously unknown purinergic mechanisms of NBP-induced metabolites and suggest ApppI as the endogenous pain inhibitor contributing to the cancer treatment with NBP.

Introduction

Patients with primary bone cancers or bone metastases of breast and prostate cancer experience high level of pain, which, in many cases, remain intractable (Mantyh, 2014; Maier *et al.*, 2016; van den Beuken-van Everdingen *et al.*, 2016).

Bisphosphonates are among the most specific bone cancer treatments available to date (Lin, 1996; Kavanagh *et al.*, 2006; Russell, 2011; Debiais, 2013; Coleman *et al.*, 2014). Bisphosphonates are divided into two main groups: (i) simple bisphosphonates without nitrogen group (non-NBP) and (ii) the most promising third generation nitrogen-containing bisphosphonates (NBP) (Frith *et al.*, 2001; Rogers *et al.*, 2011). NBPs also have an anti-nociceptive effect (Kavanagh *et al.*, 2006; Fujita *et al.*, 2009) which contributes to their therapeutic effect (Abe *et al.*, 2011; Maier *et al.*, 2016). However, the mechanisms of NBP analgesia remain unclear. We have previously shown, that NBP zoledronate inhibition of farnesyl-diphosphate synthase (FPPS) (Mönkkönen *et al.*, 2006a; Räikkönen *et al.*, 2009, 2010, 2011) induces the formation of the ATP-analogue ApppI, which can produce a toxic effect on osteoclasts and tumor cells (Lehenkari *et al.*, 2002; Green, 2004; Mönkkönen *et al.*, 2006a). However, the interaction of ApppI with the nociceptive system has not been characterized. Since ApppI structurally resembles the anti-nociceptive diadenosine polyphosphates (Viatchenko-Karpinski *et al.*, 2016), we investigated the effects of the NBP induced derivative ApppI on the activity of the nociceptive receptors P2X2, P2X3 and P2X7.

P2X3 receptors implicated in neuropathic (McGaraughty *et al.*, 2003; Chen *et al.*, 2005) and inflammatory pain (Cockayne *et al.*, 2000; Souslova *et al.*, 2000) are almost exclusively expressed in nociceptive neurons (Chen *et al.*, 1995; Lewis *et al.*, 1995). Notably, they are expressed in terminals of C- and Aδ-fibers innervating the bone (Hukkanen *et al.*, 1992; Mach *et al.*, 2002; Kaan *et al.*, 2010; Falk *et al.*, 2012; Zhao and Levy, 2014). There is abundant evidence of the involvement of P2X3 receptors in cancer pain (Kaan *et al.*, 2010; Falk *et al.*, 2012; Hansen *et al.*, 2012; Wu *et al.*, 2012; Burnstock and Di Virgilio, 2013). Interestingly, unlike in rodent models, P2X3 receptor subtype in human nociceptive neurons of the dorsal root ganglion (DRG) do not express heterotrimeric functional receptors with P2X2 subunits (Serrano *et al.*, 2012) meaning that homomeric P2X3 is the main receptor involved in nociception in bone cancer. The P2X3 and P2X2/3 receptor antagonist A-317491 attenuated bone cancer-induced pain in mice transiently, but had no effect in the late stage of the malignant process

(Hansen *et al.*, 2012). The increased expression of P2X3 receptors in CGRP containing nerve fibers during tumor growth also suggests a role for ATP receptors in cancer-related pain (Gilchrist *et al.*, 2005). Another study also found that P2X3 receptors are functionally up-regulated in DRGs in rat model of bone cancer (Wu *et al.*, 2012).

Growing evidence suggests that cancer-related bone pain is associated with osteoclast activation (Luger *et al.*, 2005; Nagae *et al.*, 2006) and Ca^{2+} misbalance. In some pathological conditions, like parathyroid hormone-related protein-mediated hypercalcemic crisis, serum Ca^{2+} reaches hypercalcemic levels rising from the normal level of ~2 mM up to 3.5 mM (Rahil and Khan, 2012; Fijorek *et al.*, 2014). There are also malignancy-associated hypercalcemia often associated with headache (Stewart, 2009; Basso *et al.*, 2011; Hu *et al.*, 2013; Goldner, 2016; Tagiyev *et al.*, 2016). Notably, serum Ca^{2+} levels can be elevated in malignancy, to 4 mM or more in most severe cases (Goldner, 2016) but in the clinic, hypercalcemia decreased 24-48 h after the NBP treatment and for 60-90 % of patients the level of serum Ca^{2+} was normalized after 4-7 days of treatment with NBP (Stewart, 2009; Endres, 2012).

Extracellular Ca^{2+} plays an important role in P2X3 signaling (Cook and McCleskey, 1997; Cook *et al.*, 1998). Thus, elevated Ca^{2+} accelerates resensitization of these receptors (Cook and McCleskey, 1997; Cook *et al.*, 1998; Giniatullin *et al.*, 2003) making them functionally more active. In contrast, Ca^{2+}-free solution prolongs ATP-evoked inactive desensitized P2X3 receptor state (Cook *et al.*, 1998; Giniatullin *et al.*, 2003).

We show here the strong Ca^{2+}-dependent inhibition of the pro-nociceptive P2X3 receptors by low nanomolar concentrations of ApppI. Our data predict that the anti-nociceptive action of ApppI should be largely enhanced when the concentration of Ca^{2+} drops in response to NBP treatment. Thus, we propose that ApppI generated by cancer treatment with NBP, like zoledronate, can contribute to pain relief via the selective inhibition of ATP-gated P2X3 receptors in the sensory neurons.

Materials and Methods

All animal use protocols were in accordance with recommendations of the Federation for Laboratory Animal Science Associations and approved by the local Institutional Animal Care and Use Committees. Wistar rats (P10-12 and P35-38) were obtained from the Animal Facilities of the University of Eastern Finland (UEF). Experiments were designed to minimize the number of animals used in research.

Cell cultures and transfection - Trigeminal and nodose ganglia cells from Wistar male rats (P10-12) were prepared as described previously (Simonetti *et al.*, 2006; Li and Schild, 2007; Yegutkin *et al.*, 2016) with minor modifications. Briefly, after decapitation, trigeminal and nodose ganglia were isolated and dissociated in the enzymatic cocktail containing collagenase, trypsin and DNAase (Sigma-Aldrich) added to F-12 media (Gibco Invitrogen) under continuous mixing (900 rpm) in Eppendorf ThermoMixer at 37°C for 15 min. After dissociation, cells were re-suspended in fresh F-12 media, centrifuged at 1000 rpm 5 min at room temperature and plated on coverslips coated with poly-L-lysine (Sigma-Aldrich). Cells were maintained in F-12 GlutaMax medium containing 10% fetal bovine serum (Gibco) and 100 U/ml penicillin and streptomycin at 37°C in a 5% CO_2 atmosphere in a humidified incubator. Cells were used for experiments 48 h after plating.

HEK293 and HEK293T cells cultures were maintained as reported previously (Fabbretti *et al.*, 2004; Viatchenko-Karpinski *et al.*, 2016) in Dulbecco's modified Eagle's medium (DMEM) (Gibco Invitrogen) supplemented with 10% FBS and antibiotics. Cells were passaged at 80% confluence. HEK cells were transiently transfected in 12 well plate (10^5 cells per well) using FugeneHD (Jindrichova *et al.*, 2011). 12 h after transfection cells were replated on cover-slips coated with poly-L-lysine (Sigma-Aldrich). Transfection was performed with cDNA encoding rP2X3 tagged with green fluorescent protein (GFP) (rP2X3-GFP), rP2X2-GFP, rP2X7-GFP and hP2X3, hP2X2, hP2X7 (GFP added separately). Sufficient receptor expression was observed in 24 h for recombinant rP2Xs and 48-72 h for hP2Xs homologue when cells were used for electrophysiological experiments.

Electrophysiological recording and solutions - Whole-cell patch-clamp recordings from HEK293 cells, trigeminal and nodose ganglia neurons were performed using HEKA-10 amplifier with HEKA PatchMaster software at the holding potential -70 mV. Glass electrodes (3-6 MΩ) filled with intracellular solution containing (in mM) : 130 CsCl, 5 $MgCl_2$, 10 HEPES, 5 EGTA, 0.5 $CaCl_2$, 2 Mg-ATP, 0.5 Na-GTP, 5 KCl, pH 7.2 adjusted by CsOH were used for the current recordings. During

experiment cells were superfused (2 ml/min) with the basic extracellular solution containing (in mM): 148 NaCl, 5 KCl, 1 $MgCl_2$, 2 CaCl2, 10 HEPES, 10 D-glucose, pH 7.4 adjusted by NaOH.

Drug delivery - P2X receptors were activated by fast (exchange time ~30 ms) agonist application using the rapid solution exchange system (RSC-200; BioLogic Science Instruments) synchronized with HEKA amplifier. Application tubes were placed ~100 - 150 μm from recordings cells. Stocks of α,β-meATP, ATP, ApppI, IPP and zoledronate (ZOL) were prepared in mQ water and diluted to the final concentrations before the experiment. Duration of agonist applications (α,β-meATP, ATP and ApppI) was typically 2 s unless otherwise indicated. For testing of ApppI, IPP, ZOL and AMP inhibitory activity, they were applied for 120 s between the test pulses.

Synthesis of ApppI and IPP - The ATP analogue ApppI was synthesized as previously reported (Weisell *et al.*, 2015). The purity of ApppI was ≥95% as determined from ^{1}H and ^{31}P NMR spectra (Weisell et. al., 2015). The purified ApppI tris(triethylammonium) salt was highly stable based on the ^{1}H and ^{31}P NMR spectra in samples stored in D_2O for ~1.5 year at room temperature. IPP was prepared from pyrophosphate tris(tetrabutylammonium) salt and isopentenyl tosylate (Kao *et al.*, 2005; Weisell *et al.*, 2015). The purity of IPP was ≥95% according to ^{1}H and ^{31}P NMR spectra (Weisell *et al.*, 2015).

Phosphate Enzymatic histochemistry - Rat hemiskulls were prepared as previously described (Yegutkin *et al.*, 2016). Briefly, the skull was cut along the sagittal suture into two halves. The brain was gently removed, leaving the dura mater intact and attached to the skull cavity. Then hemiskulls were placed in the aerated with 5 % CO_2/95 % O_2 artificial cerebrospinal fluid (ACSF) containing (in mM): 5 KCl, 119; NaCl, 18; glucose, 2.7; CaCl2, 0.5; MgCl, 1.1; NaH2PO4, 30; NaHCO3, pH 7.4. For evaluation of ApppI and ATP degradation a modification of the lead nitrate ($Pb(NO_3)_2$) method was used (Mercier *et al.*, 2012). In brief, after 30 min washing in aired ACSF, hemiskulls were washed with Trizma-maleate buffer (TMB; 40 mM Trizma® maleate; Sigma-Aldrich) and then pre-incubated for 45 min in Trizma-maleate sucrose buffer (TMSB with 0.25 M sucrose, pH 7,4) containing the alkaline phosphatase inhibitor levamisole (2 mM, Sigma-Aldrich). For the next 40 min hemiskulls were incubated with ATP or ApppI (both 300 μM) in TMSB-buffered solutions with freshly added 2 mM $Pb(NO_3)_2$. following washing in TMB. For blank specimens the same amount of the incubation medium was used. Samples treated with 0.5% $(NH_4)_2S$ (Sigma-Aldrich) formed the lead orthophosphate precipitates presented as brown deposits. After 3 washings in TMSB stained meninges were carefully

removed from hemiskulls and mounted on the glass slides coated with poly-lysine (Polysine®; Thermo-Scientific). Slides were mounted with Aquatex mounting medium (Merck). Olympus BX60 microscope with Olympus DP71 camera with PlanC 4×/0.10 or UPlanFL 10×/0.30 objective (Olympus) was used for acquiring images. All images were taken with standard settings for further analysis with the CorelDRAW Graphics Suite v.17 software.

For the quantification of histochemical images, the intensity of the signal was evaluated in each stained sample from ROI (region of the interest) located in similar areas around meningeal vessels with the same diameter (~60-95 µm).

ATP luminescence assay - ATP release from the trigeminal ganglion cells (obtained from P10-12 rats) was measured by the ATPlite Luminescence Assay System by PerkinElmer (Cat. No. 6016941 Waltham, Massachusetts). Cells were cultured in a 24 well plate for 48 h. Then growth media was changed for fresh (control) or for fresh media containing 100 µM zoledronate. After 24 hours of treatment cells were washed and bathing media was changed for the basic salt solution (BSS) containing (in mM): 152, NaCl, 2.5, KCl, 2, $CaCl_2$, 1, $MgCl_2$, 10, glucose, 10, HEPES pH 7.4. The supernatant was collected and used for the ATP assay. The assay was performed following the ATP-lite assay kit protocol instructions using Costar® white polystyrene 96-well cell plates (Corning Inc, Corning). Luminescence was measured with a microplate reader POLARstar OPTIMA (BMG LABTECH GmbH).

Statistical Data analysis - For patch clamp data analysis we used the HEKA FitMaster software. Further analysis was performed by using Origin 8.5 (OriginLab). Significance of differences was tested with the paired two-tailed Student's t-test. Dose-response fitting was made by using the Hill function. Data presented as mean ± SEM. $p < 0.05$ level was accepted as significant.

Results

Agonist activity of ApppI - First, we investigated the agonist activity of ApppI on rat recombinant P2X3 receptors expressed in HEK cells in comparison with responses induced by the full agonist of P2X3, α,β-meATP. We found that ApppI was able to activate P2X3 receptors only in relatively high concentrations. Fig 1 illustrates the typical responses of two agonists both applied for 2 s in 10 μM concentration (Fig 1B) and the dose-response curve for agonist activity of ApppI (EC_{50} = 16.4±0.9 μM, n=7, Fig 1C). One distinguishing property of the P2X3 receptor is the fast (in millisecond range) desensitization in the continuous presence of agonist (Chen *et al.*, 1995; Lewis *et al.*, 1995; Cook and McCleskey, 1997; Jiang *et al.*, 2003). In our experiments, both α,β-meATP and ApppI induced desensitizing currents (Fig 1B). However, the time of recovery from desensitization of P2X3 receptors was longer in the case of ApppI. Thus, the paired-pulse protocol with variable intervals (5-120 s) indicated that the signal activated by ApppI recovered only to 68.4±1.2 % in 2 min (n=4, Fig 1D), whereas recovery in this interval was almost complete for α,β-meATP (Fig 1B). In summary, membrane currents activated by 10 μM ApppI were nearly 10-times lower in amplitude than currents induced by similar concentration of α,β-meATP (Fig 1A). This indicated that ApppI is only a partial agonist of P2X3 receptors.

ApppI-induced inhibition of P2X3 receptors - Second, we evaluated the ability of ApppI to induce a high-affinity desensitization (HAD) of P2X3 receptors leading to inhibitory and, therefore, to anti-nociceptive effect (Giniatullin *et al.*, 2008; Viatchenko-Karpinski *et al.*, 2016). Thus, we tested the different concentrations of ApppI to determine its inhibitory potency on rP2X3 receptors. In control, a paired application of 10 μM α,β-meATP for 2 s with 120 s interval produced membrane currents with similar amplitude (Fig 2A). We found, that even 10 nM ApppI applied for 120 s between two α,β-meATP test pulses was able to inhibit P2X3 receptor mediated currents to 36±8 % of control values (p=0.0013, n=10, Fig 2B). ApppI applied at higher 100 nM concentration inhibited test currents to 15.4±3.9 % of control values (p=0.02, n=4) whereas 1 μM ApppI reduced the α,β-meATP-induced currents to 7.1±3.9 % (p=0.03, n=4). Using the same protocol, we also tested the inhibitory potency of 10 nM ApppI, when P2X3 receptors are activated by their natural agonist ATP (Fig 2C). We found, that 10 nM ApppI significantly inhibited ATP-induced P2X3 currents to 42.2±4 % (n=12, p=0.018, Fig 2D)

which was very similar to results obtained with α,β-meATP. Pooled data for the inhibitory action of ApppI on α,β-meATP- and ATP-evoked currents are shown in Fig 2E.

Further, to characterize the inhibitory action of ApppI, we constructed the dose-response curve for α,β-meATP in control and in presence of 10 nM ApppI. We found that 10 nM ApppI strongly decreased currents induced by different concentrations of α,β-meATP indicating reduced efficacy without significant changes in affinity. Thus, the EC_{50} for α,β-meATP induced currents was 1.10±0.03 μM in control (n=14) and 1.16±0.02 μM in ApppI (n=5, p>0.05, Fig 2F). These results indicated that ApppI is a non-competitive antagonist consistent with the desensitizing mechanism of its inhibitory action.

Ca^{2+}-dependence of the inhibitory action of ApppI - Since bone cancer is often associated with disturbances of Ca^{2+} homeostasis, we tested the action of ApppI in different concentrations of extracellular Ca^{2+}. We found that in low (0.2 mM) concentration of extracellular Ca^{2+}, 10 nM ApppI had the strongest depressant action on rP2X3 receptors (to 12±3 % of control, p=0.0002, n=14, Fig 3A,C). Lower inhibition was observed in 4 mM Ca^{2+} (to 68±8 %, p=0.035, n=4, Fig 3C). In sharp contrast, in high (10 mM) concentration of extracellular Ca^{2+} (which corresponds to severe hypercalcemia) we did not observe significant current suppression by ApppI (86±10 %, p>0.1, n=7, Fig 3B,C).

Selectivity of ApppI action on P2X3 subtype - To determine the specificity of ApppI action on pro-nociceptive P2X3 receptors we tested the action of this agent on rP2X2 receptors expressed in HEK293 cells. We did not detect any agonist activity of the relatively high (10 μM) concentration of ApppI on rP2X2 receptors, although we did observe a large response with 10 μM ATP (n=4, Fig 4A). We also did not observe any inhibitory effect of ApppI on rP2X2 receptors (n=4, Fig 4B). Likewise, we observed neither agonist, nor antagonist (inhibitory) action of ApppI on rP2X7 receptors (n=4, Fig 4C,D). These data suggest that ApppI acts specifically on P2X3 receptors. We further investigated the possibility that ApppI interfere with hP2X7 and hP2X2 receptor subtypes. We used similar protocols as for rP2X2 and rP2X7 receptors to evaluate both agonist and inhibitory action of ApppI. For stronger stimulation of the hP2X7 receptors, we used 1 mM ATP (Fig 4 G, H). As with the rat receptors we found neither agonist, nor inhibitory effect of ApppI on hP2X7 and hP2X2 receptors (Fig 4 C, D and G,H), suggesting again that ApppI is selective for P2X3 subunit containing receptors both in rat and human species.

We compared currents activated by α,β-meATP in trigeminal and nodose ganglia as the nodose neurons, responsible for the visceral pain, express preferentially heteromeric P2X2/3 subunits which produce slow currents with little desensitization (Viatchenko-Karpinski *et al.*, 2016). Trigeminal ganglion nociceptors take part in bone innervations, in particular, they supply the cranial periosteum (Zhao and Levy, 2014). We found that fast desensitizing currents activated with α,β-meATP in trigeminal ganglion neurons were potently inhibited by 10 nM ApppI (to 44±4 %, p=0.0007, n=17, Fig 5A). In contrast, slow currents in nodose ganglion neurons, were almost insensitive to this treatment (90.4±3.4 %, p>0.1, n=8, Fig 5B). These data also suggest selectivity of ApppI for homomeric P2X3 receptors.

Consistent with the data from rat recombinant P2X3 receptors, we observed a strong Ca^{2+}-dependent inhibitory action of ApppI on native rP2X3 receptors in trigeminal neurons. Thus, in low (0.2 mM) Ca^{2+} concentration the test currents were suppressed by 10 nM ApppI to 9.0±4.1 % (p=0.05, n=7) whereas in physiological concentration of Ca^{2+} (2 mM) α,β-meATP currents were suppressed only to 44% of control value. In conditions mimicking hypercalcemia (10 mM), we detected no inhibitory action of ApppI on trigeminal neurons (87.7±4.9 %, p>0.5, n=10, Fig 5C).

ApppI action on human P2X3 homologue - For translational aspects and to explore if this action is conserved in different species, it was interesting to study the inhibitory effect of low nanomolar ApppI on hP2X3 receptors. Interestingly, in physiological Ca^{2+} concentration in hP2X3 receptors we found a very strong depressant effect of 10 nM ApppI comparing to rat homologue (depression to 2.7±1.0 %, p=0.02, n=8, Fig 6A,C). Such strong effect of low concentrations was consistent with potential role of endogenous ApppI in human sensory neurons. Next, as with rP2X3 receptors, we characterized ApppI inhibition of hP2X3 receptors in conditions mimicking hypercalcemia (modeled with 10 mM Ca^{2+}). As expected, the inhibitory effect of 10 nM ApppI was almost fully eliminated in this hypercalcemia-like condition (84±4%, n=14, p>0.05, Fig 6B,C). Thus, we confirmed the strong Ca^{2+} dependence of the ApppI inhibition both in rP2X3 and hP2X3 receptors.

No direct effect of ApppI metabolites and zoledronate – In order to explore if the inhibitory action of ApppI required the full molecule of ApppI or if it was due to ApppI metabolites, which could exert their own physiological effect, we tested the action of IPP and AMP on P2X3 receptors. The same protocol of drug application, as for ApppI, was used for this aim. However, administration of 1 μM IPP

JPET Fast Forward. Published on April 12, 2017 as DOI: 10.1124/jpet.116.238840
This article has not been copyedited and formatted. The final version may differ from this version.

and 1 μM AMP on P2X3 receptors did not produce any inhibitory effect (Fig 7 C,D). Next, we investigated whether the inducer of ApppI zoledronate (Mönkkönen *et al.*, 2006b) can directly inhibit P2X3 receptors. We found that 10 μM zoledronate did not affect the function of P2X3 receptors (Fig 7E), suggesting the lack of the direct action of this NBP on the P2X3 receptor (Fig 7F). However, using the ATP-lite Luminescence Assay System, we found that zoledronate was able to induce the release of purines from cells to the extracellular medium. Thus, 100 μM zoledronate applied for 24 h to trigeminal neuronal culture significantly increased the concentration of extracellular ATP from 0.70 ± 0.26 nM to 3.2 ± 0.4 nM (n=12, n=6; p=0.018, Fig 7G) suggesting similar release of endogenous ApppI.

ApppI biodegradation – As many endogenous polyphosphates are quickly degraded in the live tissues by multiple nucleotidases (Yegutkin *et al.*, 2008, 2016), next we investigated the intensity of ApppI hydrolysis in rat meninges. For that purpose, we used the lead nitrate method, based on the generation of lead orthophosphate precipitation in the course of nucleotidase activity (Yegutkin *et al.*, 2008) which we recently optimized for application in transparent rat meninges (Yegutkin *et al.*, 2016). We performed this labelling to evaluate the speed of ApppI degradation in comparison with ATP. Precipitates were clearly visualized in meninges as brown deposits, around main arteries (Yegutkin *et al.*, 2016) which is the main site for migraine pain generation (Olesen *et al.*, 2009; Zakharov *et al.*, 2015). From comparison of images in Fig 8 A, B and C it is clear that the labelling was very weak in control (without added purines), stronger with of 300 μM ApppI and very intense in the case of 300 μM ATP indicating the very fast degradation of phosphates from the latter compound. Pooled data are presented for this test in Fig 8D (n=4 for all cases). These results revealed the relative stability of ApppI versus ATP suggesting a longer effect of the former on P2X3 receptors.

Discussion

The main finding of this study is that the NBP-induced ATP analogue ApppI shows a very strong and selective inhibitory effect on pro-nociceptive P2X3 receptors. Relative stability and slow resensitization of receptors interacting with this compound are favoring the inhibitory action of endogenous ApppI. We also suggest that reducing the level of extracellular Ca^{2+} during bone tumor treatment with NBP, should promote the anti-nociceptive effect of ApppI on P2X3 receptors.

Low agonist and high antagonist activity of ApppI on P2X3 receptors - We show here the strong inhibition of pain transducing P2X3 receptors by low nanomolar concentration of ApppI in trigeminal neurons and transfected HEK293 cells. Our pharmacological testing with a wide range of ApppI concentrations indicated this ATP analogue to be only a weak and partial agonist of ATP-gated P2X3 receptors. Indeed, even in saturating concentrations, the currents activated by ApppI were about 20% of the currents induced by the full agonist of P2X3 receptors α,β-meATP. In contrast, ApppI demonstrated the ability to inhibit P2X3 receptors in impressively low nanomolar concentrations. Thus, the concentration of ApppI needed to inhibit this receptor type is approximately 10000-times lower than the concentration required for activation. ApppI inhibition is most likely due to high affinity desensitization (Sokolova *et al.*, 2006), which is also observed with ATP (Sokolova *et al.*, 2006; Giniatullin and Nistri, 2013). However, ATP is a full P2X3 agonist with limited stability, while the stability ApppI appears to be much higher, a property suggesting it is able to induce prolonged inhibitory anti-nociceptive action. In a previous study we characterized synthetic Ap_nA-analogues with comparable inhibitory action on hP2X3 receptors and anti-nociceptive action *in vivo* (Viatchenko-Karpinski *et al.*, 2016), however, ApppI presents even better characteristics as more strong inhibitory anti-nociceptive agent.

Selectivity of ApppI action - High selectivity is essential for a potential analgesic agent. This study reveals that the action of ApppI on the P2X3 receptor is highly selective and acts as such. Whereas the ApppI metabolite AMP can act on adenosine A1 receptors (Rittiner *et al.*, 2012) and IPP is known to inhibit TRPV3 and TRPA1 channels (Bang *et al.*, 2011), they did not show, in our study, any activity on the P2X3 receptor. Notably, as the other indicator of selectivity, ApppI did not show any agonist or antagonist activity on either human or rP2X2 and rP2X7 receptor subtypes. Interestingly and important for translational aims, the action of ApppI on hP2X3 was even stronger than on rat homologue.

We also found that the inducer of ApppI, the NBP zoledronate, did not exert any direct effect on the pro-nociceptive P2X3 receptors, indicating that this bisphosphonate might produce an analgesic effect indirectly, through generation of endogenous ApppI.

Ca^{2+}-dependence of ApppI action and the role of P2X3 receptors in cancer pain - One specific property of ApppI activity found in the current study was that the inhibition of P2X3 receptors was dramatically dependent on the level of extracellular Ca^{2+}. Importantly, level of Ca^{2+} is increased in many bone cancers (Stewart, 2009; Basso *et al.*, 2011; Coleman *et al.*, 2014) whereas the concentration of this

cation is decreasing to the normal level during NBP anti-cancer treatment (Dodwell *et al.*, 1992; Stewart, 2009; Basso *et al.*, 2011). We showed, in this study, that the ApppI inhibition of P2X3 receptors is almost absent in high level of extracellular Ca^{2+} but very pronounced at low concentrations of this cation. Important for translational purposes, the strong inhibition of hP2X3 receptors was observed in physiological concentrations of extracellular Ca^{2+} but was eliminated in hypercalcemia-like conditions. Thus, we suggest that the painful stimuli resulting from activation of P2X3 receptors in bone cancer tissues (Hukkanen *et al.*, 1992; Kaan *et al.*, 2010; Falk *et al.*, 2012; Burnstock and Di Virgilio, 2013; Zhao and Levy, 2014) are amplified by the high level of extracellular Ca^{2+} (Giniatullin *et al.*, 2003; Petrenko *et al.*, 2011; Giniatullin and Nistri, 2013). During NBP treatment, NBP-induced endogenous ApppI, assisted by normalized (reduced from hypercalcemia) Ca^{2+} concentrations, could inactivate P2X3 receptors. The schematic presentation of these findings is depicted in Fig 9. ATP-activated P2X3 receptors, the most common type of nociceptors expressed in sensory neurons (Chen *et al.*, 1995; Lewis *et al.*, 1995; Simonetti *et al.*, 2006) are activated by ATP released from multiple cellular sources including cancer cells (Fig 9A). Elevated Ca^{2+}, resulting from bone cancer, helps to keep activity of P2X3 receptors at high level. We propose that cancer treatment with NBP not only generates endogenous ApppI but also sensitizes sensory neurons to ApppI inhibition via reduced level of extracellular Ca^{2+} (Fig 9B). Importantly, previous studies already showed that the antagonists of P2X3 receptors was able to decrease bone pain (Mach *et al.*, 2002; Falk *et al.*, 2012) which supports the proposed purinergic mechanism for pain relief.

This study clarifies previously unexplored mechanisms of anti-nociception induced by NBP and proposes the analgesic role of the endogenous ATP analogue generated during bone cancer treatment. We suggest that pain relief derived from NBP includes ApppI-induced inactivation of the P2X3 receptors, further amplified by a lowered level of extracellular Ca^{2+}. The high efficiency of ApppI in inactivation of pain receptors can help to design the new types of anti-nociceptive agents to manage painful bone cancer and bone metastases.

Conflict of interest. The authors declare that they have no conflict of interests.

Authors contribution:

Research design and general supervision: Giniatullin, Määttä and Mönkkönen.

Conducted experiments: Ishchenko, Shakirzyanova, Giniatullina, Skorinkin.

Synthesis of ApppI and IPP: Turhanen.

Performed data analysis: Ishchenko, Shakirzyanova, Giniatullina

Drafted manuscript: Ishchenko, Giniatullin.

Edited and revised manuscript: Ishchenko, Shakirzyanova, Giniatullina, Skorinkin, Bart, Turhanen, Määttä, Mönkkönen and Giniatullin.

Approved final manuscript: Ishchenko, Shakirzyanova, Giniatullina, Skorinkin, Bart, Turhanen, Määttä, Mönkkönen and Giniatullin.

References

Abe Y, Iba K, Takada J, Wada T, and Yamashita T (2011) Improvement of pain and regional osteoporotic changes in the foot and ankle by low-dose bisphosphonate therapy for complex regional pain syndrome type I: a case series. *J Med Case Rep* **5**:349.

Bang S, Yoo S, Yang TJ, Cho H, and Hwang SW (2011) Isopentenyl pyrophosphate is a novel antinociceptive substance that inhibits TRPV3 and TRPA1 ion channels. *Pain* **152**:1156–1164, International Association for the Study of Pain.

Basso U, Maruzzo M, Roma A, Camozzi V, Luisetto G, and Lumachi F (2011) Malignant hypercalcemia. *Curr Med Chem* **18**:3462–7.

Burnstock G, and Di Virgilio F (2013) Purinergic signalling and cancer. *Purinergic Signal* **9**:491–540.

Chen C-C, Akopian AN, Sivilottit L, Colquhoun D, Burnstock G, and Wood JN (1995) A P2X purinoceptor expressed by a subset of sensory neurons. *Nature* **377**:428–431.

Chen Y, Li G-W, Wang C, Gu Y, and Huang L-YM (2005) Mechanisms underlying enhanced P2X receptor-mediated responses in the neuropathic pain state. *Pain* **119**:38–48.

Cockayne DA, Hamilton SG, Zhu Q-M, Dunn PM, Zhong Y, Novakovic S, Malmberg AB, Cain G, Berson A, Kassotakis L, Hedley L, Lachnit WG, Burnstock G, McMahon SB, and Ford APDW (2000) Urinary bladder hyporeflexia and reduced pain-related behaviour in P2X3-deficient mice. *Nature* **407**:1011–1015, Nature Publishing Group.

Coleman R, Body JJ, Aapro M, Hadji P, Herrstedt J, and ESMO Guidelines Working Group (2014) Bone health in cancer patients: ESMO Clinical Practice Guidelines. *Ann Oncol* **25 suppl 3**:iii124–34, Oxford University Press.

Cook SP, and McCleskey EW (1997) Desensitization, recovery and Ca2+-dependent modulation of ATP-gated P2X receptors in nociceptors. *Neuropharmacology* **36**:1303–1308.

Cook SP, Rodland KD, and McCleskey EW (1998) A memory for extracellular Ca2+ by speeding recovery of P2X receptors from desensitization. *J Neurosci* **18**:9238–44, Society for Neuroscience.

Debiais F (2013) Bone targeting agents: bisphosphonates. *Bull Cancer* **100**:1199–206.

Dodwell DJ, Howell A, Morton AR, Daley-Yates PT, and Hoggarth CR (1992) Infusion rate and pharmacokinetics of intravenous pamidronate in the treatment of tumour-induced hypercalcaemia. *Postgrad Med J* **68**:434–9, The Fellowship of Postgraduate Medicine.

Endres DB (2012) Investigation of hypercalcemia. *Clin Biochem* **45**:954–963, Elsevier B.V.

Fabbretti E, Sokolova E, Masten L, D'Arco M, Fabbro A, Nistri A, and Giniatullin R (2004) Identification of Negative Residues in the P2X3 ATP Receptor Ectodomain as Structural Determinants for Desensitization and the Ca2+-sensing Modulatory Sites. *J Biol Chem* **279**:53109–53115, American Society for Biochemistry and Molecular Biology.

Falk S, Uldall M, and Heegaard AM (2012) The role of purinergic receptors in cancer-induced bone pain. *J Osteoporos* **2012**.

Fijorek K, Püsküllüoğlu M, Tomaszewska D, Tomaszewski R, Glinka A, and Polak S (2014) Serum potassium, sodium and calcium levels in healthy individuals - literature review and data analysis. *Folia Med Cracov* **54**:53–70.

Frith JC, Mönkkönen J, Auriola S, Mönkkönen H, and Rogers MJ (2001) The molecular mechanism of action of the antiresorptive and antiinflammatory drug clodronate: evidence for the formation in vivo of a metabolite that inhibits bone resorption and causes osteoclast and macrophage apoptosis. *Arthritis Rheum* **44**:2201–10.

Fujita T, Ohue M, Fujii Y, Miyauchi A, and Takagi Y (2009) Comparison of the analgesic effects of bisphosphonates: Etidronate, alendronate and risedronate by electroalgometry utilizing the fall of skin impedance. *J Bone Miner Metab* **27**:234–239.

Gilchrist LS, Cain DM, Harding-Rose C, Kov AN, Wendelschafer-Crabb G, Kennedy WR, and Simone DA (2005) Re-organization of P2X3 receptor localization on epidermal nerve fibers in a murine model of cancer pain. *Brain Res* **1044**:197–205.

Giniatullin R, and Nistri A (2013) Desensitization properties of P2X3 receptors shaping pain signaling. *Front Cell Neurosci* **7**:245, Frontiers Media SA.

Giniatullin R, Nistri A, and Fabbretti E (2008) Molecular mechanisms of sensitization of pain-transducing P2X3 receptors by the migraine mediators CGRP and NGF. *Mol Neurobiol* **37**:83–90.

Giniatullin R, Sokolova E, and Nistri A (2003) Modulation of P2X3 receptors by Mg2+ on rat DRG neurons in culture. *Neuropharmacology* **44**:132–140.

Goldner W (2016) Cancer-Related Hypercalcemia. *J Oncol Pract* **12**:426–32.

Green JR (2004) Bisphosphonates: preclinical review. *Oncologist* **9 Suppl 4**:3–13, AlphaMed Press.

Hansen RR, Nasser A, Falk S, Baldvinsson SB, Ohlsson PH, Bahl JMC, Jarvis MF, Ding M, and Heegaard A-M (2012) Chronic administration of the selective P2X3, P2X2/3 receptor antagonist, A-317491, transiently attenuates cancer-induced bone pain in mice. *Eur J Pharmacol* **688**:27–34.

Hu MI, Glezerman I, Leboulleux S, Insogna K, Gucalp R, Misiorowski W, Yu B, Ying W, and Jain RK (2013) Denosumab for patients with persistent or relapsed hypercalcemia of malignancy despite recent bisphosphonate treatment. *J Natl Cancer Inst* **105**:1417–1420.

Hukkanen M, Konttinen YT, Rees RG, Santavirta S, Terenghi G, and Polak JM (1992) Distribution of nerve endings and sensory neuropeptides in rat synovium, meniscus and bone. *Int J Tissue React* **14**:1–10.

Jiang L-H, Kim M, Spelta V, Bo X, Surprenant A, and North RA (2003) Subunit arrangement in P2X receptors. *J Neurosci* **23**:8903–10, Society for Neuroscience.

Jindrichova M, Khafizov K, Skorinkin A, Fayuk D, Bart G, Zemkova H, and Giniatullin R (2011) Highly conserved tyrosine 37 stabilizes desensitized states and restricts calcium permeability of ATP-gated P2X3 receptor. *J Neurochem* **119**:676–85.

Kaan TKY, Yip PK, Patel S, Davies M, Marchand F, Cockayne DA, Nunn PA, Dickenson AH, Ford APDW, Zhong Y, Malcangio M, and McMahon SB (2010) Systemic blockade of P2X3 and P2X2/3 receptors attenuates bone cancer pain behaviour in rats. *Brain* **133**:2549–2564.

Kao C, Kittleman W, Zhang H, Seto H, and Liu H (2005) Stereochemical analysis of isopentenyl

diphosphate isomerase type II from Staphylococcus aureus using chemically synthesized (S)- and (R)-[2-2H]isopentenyl diphosphates. *Org Lett* **7**:5677–80.

Kavanagh KL, Guo K, Dunford JE, Wu X, Knapp S, Ebetino FH, Rogers MJ, Russell RGG, and Oppermann U (2006) The molecular mechanism of nitrogen-containing bisphosphonates as antiosteoporosis drugs. *Proc Natl Acad Sci U S A* **103**:7829–34, National Academy of Sciences.

Lehenkari PP, Kellinsalmi M, Näpänkangas JP, Ylitalo K V, Mönkkönen J, Rogers MJ, Azhayev A, Väänänen HK, and Hassinen IE (2002) Further insight into mechanism of action of clodronate: inhibition of mitochondrial ADP/ATP translocase by a nonhydrolyzable, adenine-containing metabolite. *Mol Pharmacol* **61**:1255–62.

Lewis C, Neidhart S, Holy C, North R, A., Buell G, and Surprenant A (1995) Coexpression of P2X2 and P2X3 receptor subunits can account for ATP-gated currents in sensory neurons. *Nature* **377**:432–435.

Li B-Y, and Schild JH (2007) Electrophysiological and pharmacological validation of vagal afferent fiber type of neurons enzymatically isolated from rat nodose ganglia. *J Neurosci Methods* **164**:75–85, NIH Public Access.

Lin JH (1996) Bisphosphonates: a review of their pharmacokinetic properties. *Bone* **18**:75–85.

Luger NM, Mach DB, Sevcik MA, and Mantyh PW (2005) Bone Cancer Pain: From Model to Mechanism to Therapy. *J Pain Symptom Manage* **29**:32–46.

Mach D., Rogers S., Sabino M., Luger N., Schwei M., Pomonis J., Keyser C., Clohisy D., Adams D., O'Leary P, and Mantyh P. (2002) Origins of skeletal pain: sensory and sympathetic innervation of the mouse femur. *Neuroscience* **113**:155–166.

Maier GS, Eberhardt C, and Kurth AA (2016) Ibandronate: The loading dose concept in the treatment of metastatic bone pain. *J Bone Oncol* **5(1)**:1–4.

Mantyh PW (2014) Bone cancer pain: from mechanism to therapy. *Curr Opin Support Palliat Care* **8(2)**:83–90, NIH Public Access.

McGaraughty S, Wismer CT, Zhu CZ, Mikusa J, Honore P, Chu KL, Lee C-H, Faltynek CR, and Jarvis MF (2003) Effects of A-317491, a novel and selective P2X3/P2X2/3 receptor antagonist, on neuropathic, inflammatory and chemogenic nociception following intrathecal and intraplantar administration. *Br J Pharmacol* **140**:1381–8, Wiley-Blackwell.

Mercier N, Kiviniemi TO, Saraste A, Miiluniemi M, Silvola J, Jalkanen S, and Yegutkin GG (2012) Impaired ATP-induced coronary blood flow and diminished aortic NTPDase activity precede lesion formation in apolipoprotein E-deficient mice. *Am J Pathol* **180**:419–28.

Mönkkönen H, Auriola S, Lehenkari P, Kellinsalmi M, Hassinen IE, Vepsäläinen J, and Mönkkönen J (2006a) A new endogenous ATP analog (ApppI) inhibits the mitochondrial adenine nucleotide translocase (ANT) and is responsible for the apoptosis induced by nitrogen-containing bisphosphonates. *Br J Pharmacol* **147**:437–45.

Mönkkönen H, Auriola S, Lehenkari P, Kellinsalmi M, Hassinen IE, Vepsäläinen J, and Mönkkönen J (2006b) A new endogenous ATP analog (ApppI) inhibits the mitochondrial adenine nucleotide translocase (ANT) and is responsible for the apoptosis induced by nitrogen-containing bisphosphonates. *Br J Pharmacol* **147**:437–45.

Nagae M, Hiraga T, Wakabayashi H, Wang L, Iwata K, and Yoneda T (2006) Osteoclasts play a part in pain due to the inflammation adjacent to bone. *Bone* **39**:1107–1115.

Olesen J, Burstein R, Ashina M, and Tfelt-Hansen P (2009) Origin of pain in migraine: evidence for peripheral sensitisation. *Lancet Neurol* **8**:679–690.

Petrenko N, Khafizov K, Tvrdonova V, Skorinkin A, and Giniatullin R (2011) Role of the ectodomain serine 275 in shaping the binding pocket of the ATP-gated P2X3 receptor. *Biochemistry* **50**:8427–36, American Chemical Society.

Rahil A, and Khan FY (2012) Humoral hypercalcemic crisis in a pregnant woman with uterine leiomyoma. *J Emerg Trauma Shock* **5**:87–9, Medknow Publications.

Rittiner JE, Korboukh I, Hull-Ryde EA, Jin J, Janzen WP, Frye S V., and Zylka MJ (2012) AMP Is an adenosine A1 receptor agonist. *J Biol Chem* **287**:5301–5309.

Rogers MJ, Crockett JC, Coxon FP, and Mönkkönen J (2011) Biochemical and molecular mechanisms of action of bisphosphonates. *Bone* **49**:34–41, Elsevier Inc.

Russell RGG (2011) Bisphosphonates: The first 40 years. *Bone* **49**:2–19.

Räikkönen J, Crockett JC, Rogers MJ, Mönkkönen H, Auriola S, and Mönkkönen J (2009) Zoledronic acid induces formation of a pro-apoptotic ATP analogue and isopentenyl pyrophosphate in osteoclasts in vivo and in MCF-7 cells in vitro. *Br J Pharmacol* **157**:427–435.

Räikkönen J, Mönkkönen H, Auriola S, and Mönkkönen J (2010) Mevalonate pathway intermediates downregulate zoledronic acid-induced isopentenyl pyrophosphate and ATP analog formation in human breast cancer cells. *Biochem Pharmacol* **79**:777–783.

Räikkönen J, Taskinen M, Dunford JE, Mönkkönen H, Auriola S, and Mönkkönen J (2011) Correlation between time-dependent inhibition of human farnesyl pyrophosphate synthase and blockade of mevalonate pathway by nitrogen-containing bisphosphonates in cultured cells. *Biochem Biophys Res Commun* **407**:663–667.

Serrano A, Mo G, Grant R, Pare M, O'Donnell D, Yu XH, Tomaszewski MJ, Perkins MN, Seguela P, and Cao CQ (2012) Differential Expression and Pharmacology of Native P2X Receptors in Rat and Primate Sensory Neurons. *J Neurosci* **32**:11890–11896, Society for Neuroscience.

Simonetti M, Fabbro A, D'Arco M, Zweyer M, Nistri A, Giniatullin R, and Fabbretti E (2006) Comparison of P2X and TRPV1 receptors in ganglia or primary culture of trigeminal neurons and their modulation by NGF or serotonin. *Mol Pain* **2**:11, SAGE Publications.

Sokolova E, Skorinkin A, Moiseev I, Agrachev A, Nistri A, and Giniatullin R (2006) Experimental and modeling studies of desensitization of P2X3 receptors. *Mol Pharmacol* **70**:373–82.

Souslova V, Cesare P, Ding Y, Akopian AN, Stanfa L, Suzuki R, Carpenter K, Dickenson A, Boyce S, Hill R, Nebenuis-Oosthuizen D, Smith AJH, Kidd EJ, Wood JN, Souslova V, Cesare P, Ding Y, Akopian AN, Stanfa L, Suzuki R, Carpenter K, Dickenson A, Boyce S, Hill R, Nebenius-Oosthuizen D, Smith AJH, and Kidd EJ (2000) Warm-coding deficits and aberrant inflammatory pain in mice lacking P2X 3 receptors. *Nature* **407**:1015–7, Nature Publishing Group.

Stewart AF (2009) Hypercalcemia Associated with Cancer. *http://dx.doi.org.ez.statsbiblioteket.dk:2048/101056/NEJMcp042806* 373–379.

Tagiyev A, Demirbilek H, Tavil B, Buyukyilmaz G, Gumruk F, and Cetin M (2016) Severe Hypercalcemia in a Child With Acute Lymphoblastic Leukemia Relapse. *J Pediatr Hematol Oncol* **38**:232–234.

van den Beuken-van Everdingen MHJ, Hochstenbach LMJ, Joosten EAJ, Tjan-Heijnen VCG, and Janssen DJA (2016) Update on Prevalence of Pain in Patients With Cancer: Systematic Review and Meta-Analysis. *J Pain Symptom Manage* **51**:1070–1090.e9.

Weisell J, Vepsäläinen J, and Turhanen PA (2015) Two strategies for the synthesis of the biologically important ATP analogue ApppI, at a multi-milligram scale. *Beilstein J Org Chem* **11**:2189–93, Beilstein-Institut.

Viatchenko-Karpinski V, Novosolova, N., Ishchenko Y, Azhar MA, Wright M, Tsintsadze V, Kamal A, Burnashev N, Miller AD, Voitenko N, Giniatullin R, and Lozovaya N (2016) Stable, synthetic analogs of diadenosine tetraphosphate inhibit rat and human P2X3 receptors and inflammatory pain. *Mol Pain* **12**:1–16.

Wu JX, Xu MY, Miao XR, Lu ZJ, Yuan XM, Li XQ, and Yu WF (2012) Functional up-regulation of P2X3 receptors in dorsal root ganglion in a rat model of bone cancer pain. *Eur J Pain* **16**:1378–1388.

Yegutkin GG, Guerrero-Toro C, Kilinc E, Koroleva K, Ishchenko Y, Abushik P, Giniatullina R, Fayuk D, and Giniatullin R (2016) Nucleotide homeostasis and purinergic nociceptive signaling in rat meninges in migraine-like conditions. *Purinergic Signal* **12(3)**:561–74.

Yegutkin GG, Jankowski J, Jalkanen S, Günthner T, Zidek W, and Jankowski V (2008) Dinucleotide polyphosphates contribute to purinergic signalling via inhibition of adenylate kinase activity. *Biosci Rep* **28**:189–94.

Zakharov A, Vitale C, Kilinc E, Koroleva K, Fayuk D, Shelukhina I, Naumenko N, Skorinkin A, Khazipov R, and Giniatullin R (2015) Hunting for origins of migraine pain: cluster analysis of

spontaneous and capsaicin-induced firing in meningeal trigeminal nerve fibers. *Front Cell Neurosci* **9**:287.

Zhao J, and Levy D (2014) The sensory innervation of the calvarial periosteum is nociceptive and contributes to headache-like behavior. *Pain* **155**:1392–400, NIH Public Access.

Foot Notes The study was supported by the Finnish Academy grant 277442.

Figure legend

Fig 1 Agonist activity of ApppI on P2X3 receptors. **(A)** Chemical structures of ApppI, synthesized and used for the experiments. Chemical structure of ApppI has been constructed using ChemBioDraw Ultra software. **(B)** Example of rP2X3 receptor mediated currents induced by application of 10 μM α,β-meATP (here and further αβ=α,β-meATP) and 10 μM ApppI to rP2X3 transfected HEK293 cells. **(C)** Dose-response curve of ApppI action on rP2X3 receptors (EC_{50}=16.37±0.94 μM, n=7). **(D)** Example of P2X3 receptor mediated desensitizing currents induced by paired application of 10 μM ApppI.

Fig 2 Inhibitory potency of ApppI on P2X3 receptors. (A) Example of current induced by10 μM α,β-meATP, applied for 2 s with interval of 120 s. Notice full recovery of the second current. **(B)** Example of the inhibitory action of 10 nM ApppI applied for 120 s between two α,β-meATP applications. **(C**) Example current induced by of 20 μM ATP, applied for 2 s with interval of 120 s. Similarly as for α,β-meATP-induced second current the ATP-induced is fully recovered in 120 s. **(D)** Example of the inhibitory action of 10 nM ApppI applied for 120 s between two ATP applications, demonstrates similar rates of ApppI inhibition for ATP and α,β-meATP-induced rP2X3 currents. **(E)** Histograms showing the inhibitory effect of different ApppI concentrations on α,β-meATP-induced currents (empty white circles, 7.1±3.9 %, p=0.03, 15.4±3.9 %, p=0.02 and 36±8 %, p=0.0013, respectively, n=4-10) and inhibitory effect of 10 nM ApppI on ATP-stimulated (black circle) rP2X3 currents (p=0.018, n=12). **(F)** Dose-response curves of α,β-meATP alone (black, EC_{50} 1.10±0.03 μM, n=14) and in presence of the 10 nM ApppI (gray, EC_{50}=1.16±0.02 μM, n=5) on rP2X3 receptors.

Fig 3 Ca^{2+}-dependent inhibitory action of ApppI on rP2X3 receptors. (A) Example of the inhibitory action of 10 nM ApppI in low (0.2 mM) extracellular Ca^{2+}. **(B)** Example of ApppI (10 nM) application in high (10 mM) extracellular Ca^{2+}. **(C)** Histograms showing Ca^{2+}-dependent action of 10 nM ApppI on rat recombinant rP2X3 receptors. p=0.0002, n=14; p=0.0013, n=10; p=0.035, n=4; p>0.1, n=7; respectively for 0.2, 2, 4 and 10 mM of extracellular Ca^{2+}.

Fig 4 Testing ApppI action on P2X2 and P2X7 receptors. (A) Example of ATP-activated rP2X2 receptor mediated currents and absence of the agonist effect of 10 μM ApppI on this receptor type (n=4).

(B) Testing the inhibitory action of 1 μM ApppI applied for 120 s on rP2X2 receptors (n=4). Notice that even this relatively high concentration of ApppI was unable to inhibit non-desensitizing rP2X2 currents. **(C)** Example of ATP-activated hP2X2 receptor mediated currents and absence of the agonist effect of 10 μM ApppI on this receptor type (n=4). **(D)** Absence of the inhibitory action of 1 μM ApppI applied for 120 s on hP2X2 receptors (n=7). **(E**) Example of ATP-activated rP2X7 receptor mediated currents showing the absence of agonist effect of 100 μM ApppI on this receptor type (n=4)**. (F)** Testing the inhibitory action of 1 μM ApppI applied for 120 s on rP2X7 receptors. Notice no effect of ApppI (n=4). **(G**) Example of ATP-mediated (1mM) hP2X7 receptor currents showing the absence of agonist effect of 100 μM ApppI on this receptor type (n=6). **(H)** Experimental trace demonstrating, no effect after 1 μM ApppI application for 120 s on hP2X7 receptors (n=8).

Fig 5 Comparing ApppI inhibition in trigeminal and nodose ganglia neurons (A) Example of α,β-meATP current inhibition by 10 nM ApppI in trigeminal ganglia neurons. **(B)** Example of lack of inhibitory effect of 10 nM ApppI on currents in nodose ganglia neurons. **(C)** Histograms presenting Ca^{2+}-dependent inhibition by 10 nM ApppI of native P2X receptors in trigeminal and nodose ganglion neurons. p=0.050, n=7; p=0.0007, n=17; p>0.5, n=10 for trigeminal ganglion in 0.2, 2, 10 mM Ca^{2+}, respectively, and p>0.1, n=8 for nodose ganglion neurons.

Fig 6 ApppI inhibition of hP2X3 subtype. (A) Example of the inhibitory action of 10 nM ApppI in physiological (2 mM) extracellular Ca^{2+}on α,β-meATP-activated currents in hP2X3 receptors. **(B**) Example of ApppI (10 nM) application in high (10 mM) extracellular Ca^{2+} on α,β-meATP-activated currents in hP2X3 receptors. Note, Ca^{2+}-dependent decrease of the ApppI inhibition on hP2X3 replicates effect on rP2X3 subtype. **(C**) Histograms showing statistics on the inhibition by 10 nM ApppI and recovery of the hP2X3-induced currents in 2 mM and 10mM of extracellular Ca^{2+} respectively (2.7±1.0 %, vs control p=0.02, n=8, empty white circles; 84±4%, n=14, p>0.5, black circles).

Fig 7 Lack of the inhibitory effect of AMP, IPP or zoledronate on P2X3 receptors. (A,B) Chemical structures of isopentenyl pyrophosphate (IPP) and zoledronate (ZOL), synthesized and used for the experiments. Chemical structures of IPP and Zoledronate have been constructed using

ChemBioDraw Ultra software. **(C-E)** Examples of action of 1 µM AMP, 1 µM IPP or 10 µM zoledronate on α,β-meATP activated currents. **(F)** Histograms represents average effects of AMP, IPP and zoledronate on P2X3 receptors ($p \geq 0.9$, n=10; $p \geq 0.8$, n=11; $p \geq 0.8$, n=13, respectively). **(G)** Histogram demonstrates ATP-Luminescent assay data, of extracellular ATP concentration significant increase from TG neurons after treatment with 100 µM ZOL during 24 h (0.70 ± 0.26 nM, n=12 in control; 3.2 ± 0.4 nM, n=6 after treatment; p=0.018).

Fig 8 Comparison of nucleotide hydrolysis of ApppI and ATP. (A-C). Images of meninges treated with vehicle, 300 µM ApppI and 300 µM ATP, respectively. The activity of nucleotidases generating phosphate due polyphosphates hydrolysis was visualized using lead nitrate and diamonium sulphide (n=5). **(D)** Histogram representing statistic of the signal intensity of the vessels colored after phosphate staining with added substances (control 28.4±2.4, n=4; ATP 221.1±8.7, n=4, $p<0.0001$; ApppI 59.6±6.3,n=4, p=0.0033)

Fig 9 Schematic presentation of potential action of NBP and ApppI on P2X3 mediated bone cancer pain. (A) Presentation of the cancer related local bone environment and potential role of P2X3 receptors in mediating bone cancer pain. Notice ATP release from cancer cells, associated hypercalcemia and Ca^{2+}-dependent persistent activation of painful P2X3 receptors in cancer state. **(B)** Cancer treatment with NBP leads to less bone resorption and lower level of extracellular Ca^{2+} which is up taken into osteoblasts. All this promotes the inhibitory action of NBP-induced ApppI on the pro-nociceptive P2X3 receptors resulting in pain relief. *Red lines indicate pro-nociceptive whereas black lines show anti-nociceptive effects.*

JPET Fast Forward. Published on April 12, 2017 as DOI: 10.1124/jpet.116.238840
This article has not been copyedited and formatted. The final version may differ from this version.

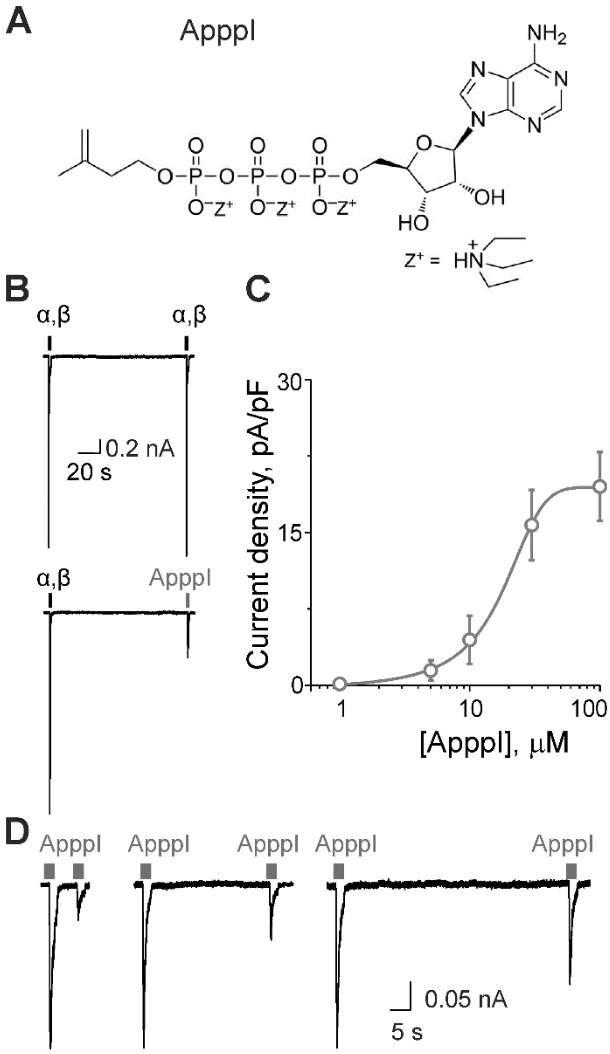

Fig 1

JPET Fast Forward. Published on April 12, 2017 as DOI: 10.1124/jpet.116.238840
This article has not been copyedited and formatted. The final version may differ from this version.

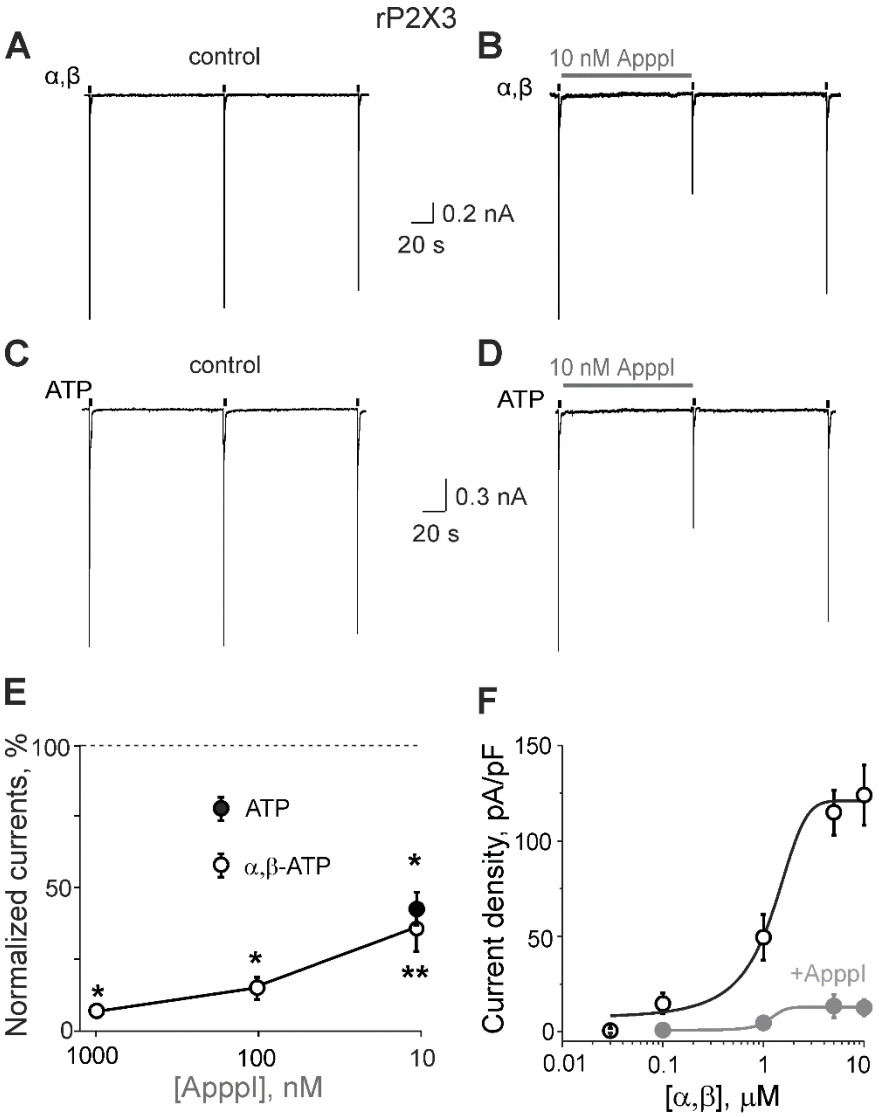

Fig 2

JPET Fast Forward. Published on April 12, 2017 as DOI: 10.1124/jpet.116.238840
This article has not been copyedited and formatted. The final version may differ from this version.

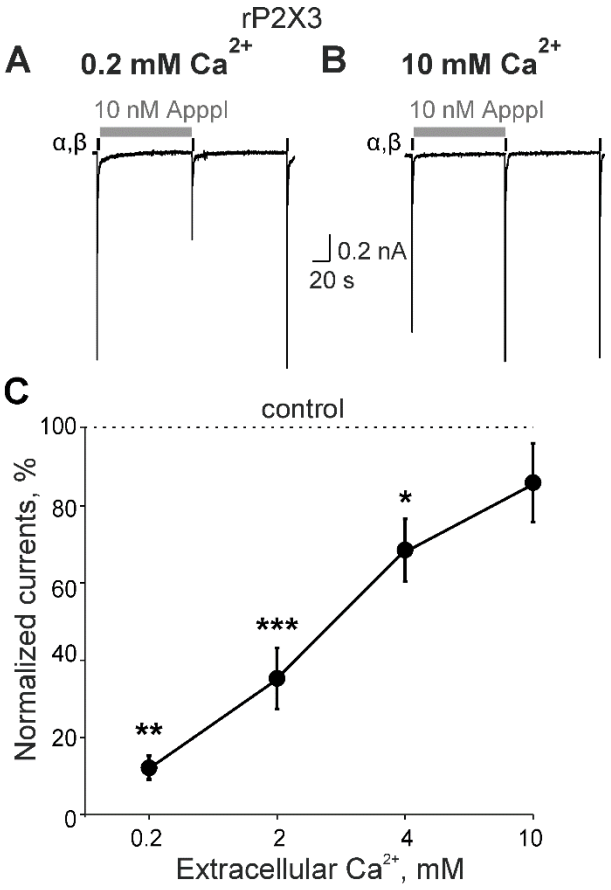

Fig 3

JPET Fast Forward. Published on April 12, 2017 as DOI: 10.1124/jpet.116.238840
This article has not been copyedited and formatted. The final version may differ from this version.

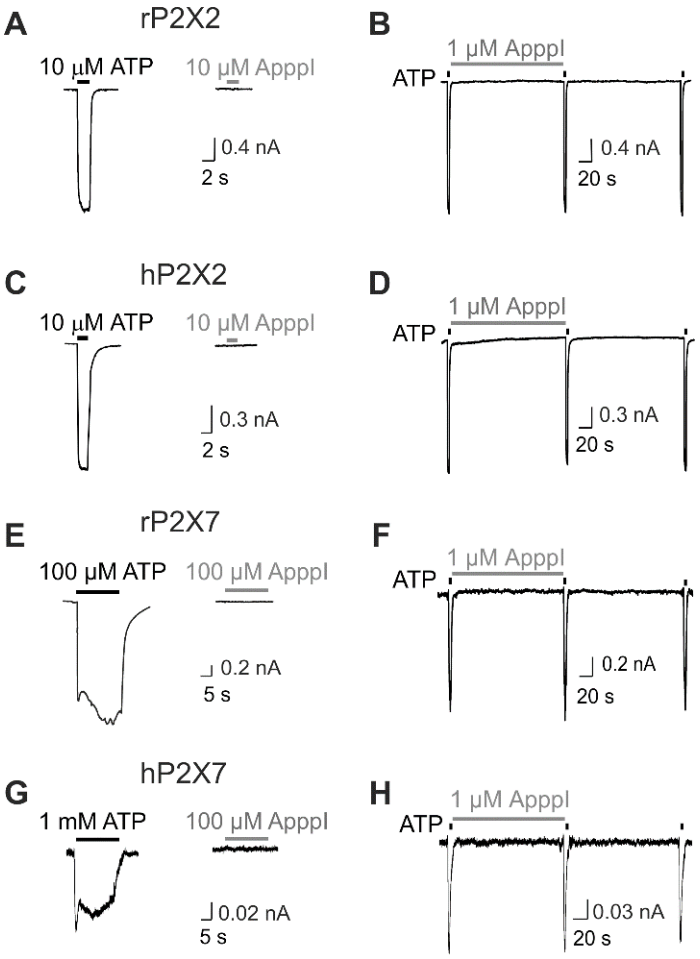

Fig 4

JPET Fast Forward. Published on April 12, 2017 as DOI: 10.1124/jpet.116.238840
This article has not been copyedited and formatted. The final version may differ from this version.

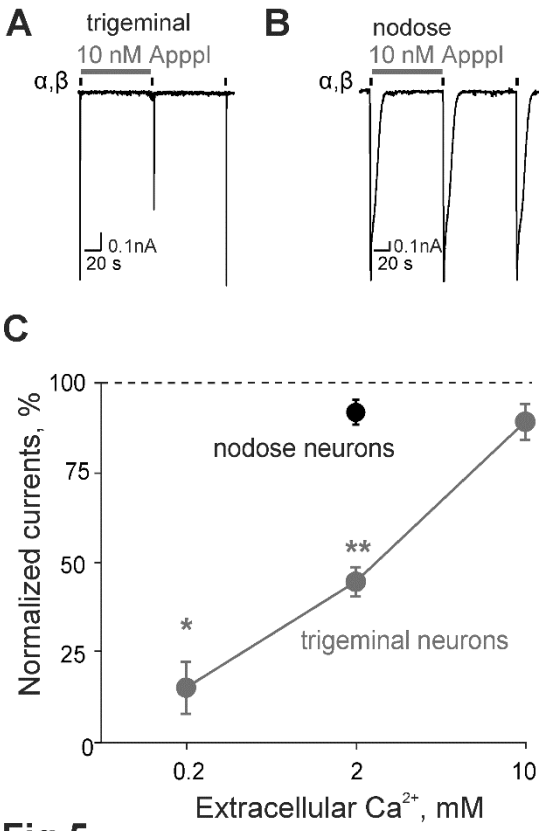

Fig 5

JPET Fast Forward. Published on April 12, 2017 as DOI: 10.1124/jpet.116.238840
This article has not been copyedited and formatted. The final version may differ from this version.

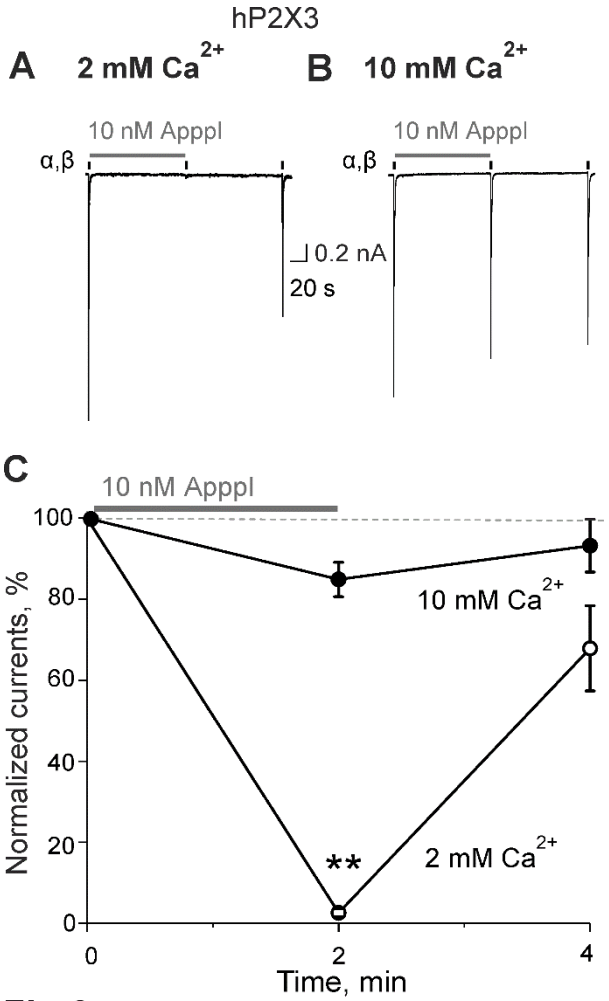

Fig 6

JPET Fast Forward. Published on April 12, 2017 as DOI: 10.1124/jpet.116.238840
This article has not been copyedited and formatted. The final version may differ from this version.

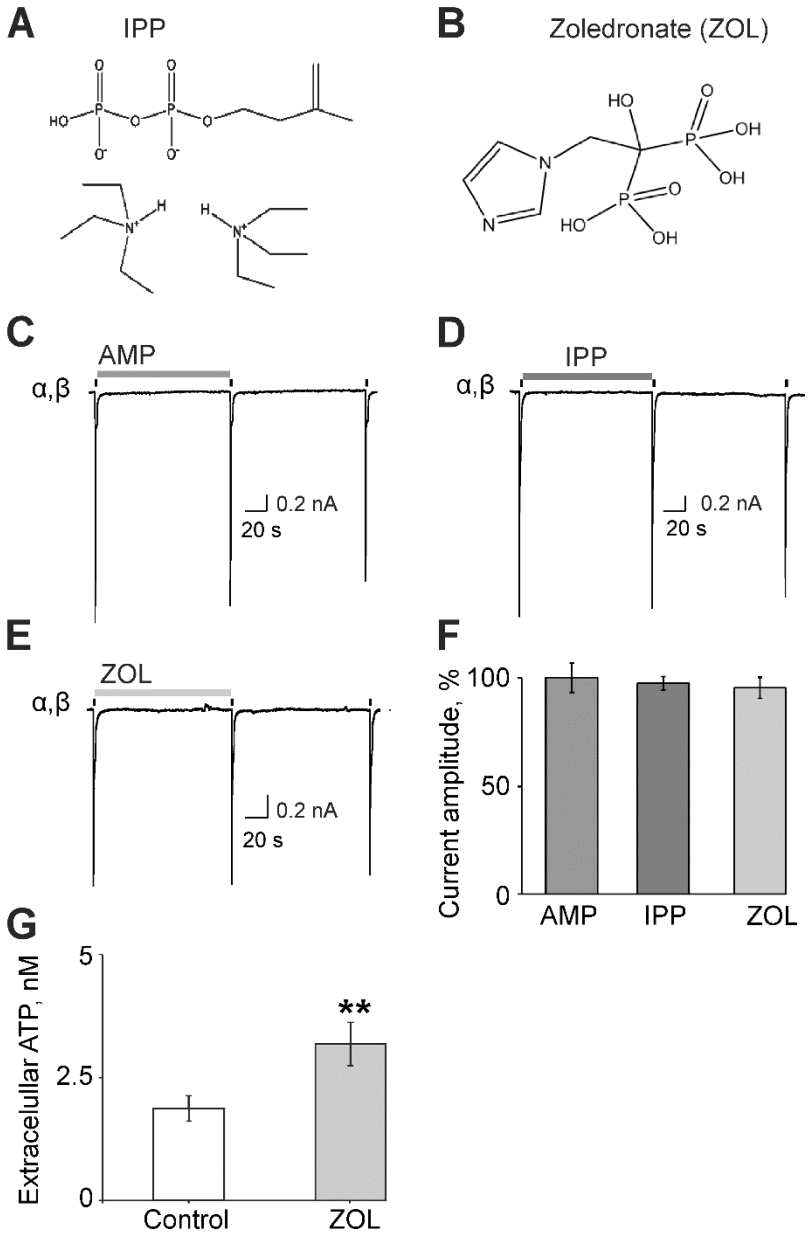

Fig 7

JPET Fast Forward. Published on April 12, 2017 as DOI: 10.1124/jpet.116.238840
This article has not been copyedited and formatted. The final version may differ from this version.

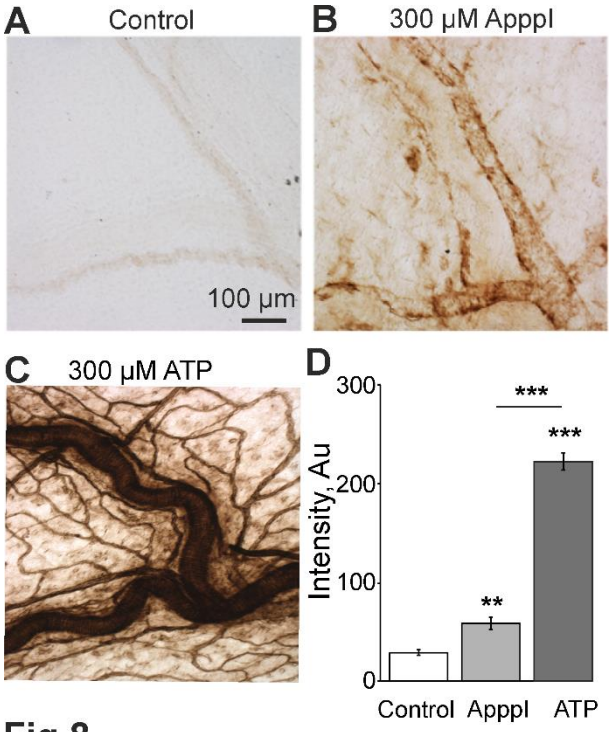

Fig 8

JPET Fast Forward. Published on April 12, 2017 as DOI: 10.1124/jpet.116.238840
This article has not been copyedited and formatted. The final version may differ from this version.

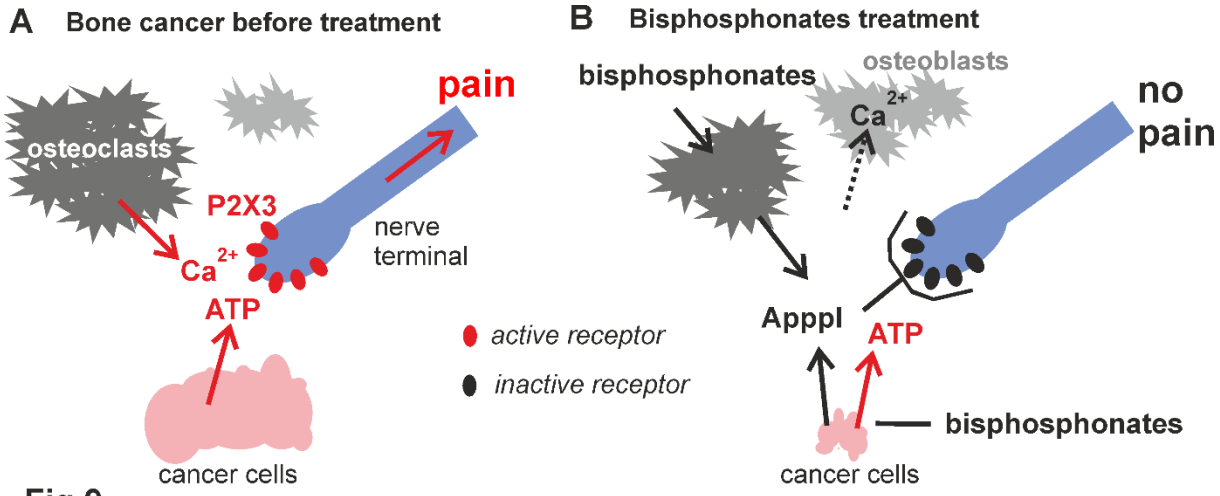

Fig 9